Physics of the Earth and Planetary Interiors, 49 (1987) 264–282
Elsevier Science Publishers B.V., Amsterdam – Printed in The Netherlands

Tensional intraplate seismicity in the Eastcentral Pacific

Douglas A. Wiens

Department of Earth and Planetary Sciences, Washington University, Saint Louis, Missouri 63130 (U.S.A.)

Emile A. Okal

Department of Geological Sciences, Northwestern University, Evanston, Illinois 60201 (U.S.A.)

(Received March 10, 1987; accepted May 3, 1987)

Wiens, D.A. and Okal, E.A., 1987. Tensional intraplate seismicity in the Eastcentral Pacific. Phys. Earth Planet. Inter., 49: 264–282.

We identify a region of enhanced intraplate seismicity west of the Mathematicians Ridge in the Eastcentral Pacific. Recent activity includes the December 2, 1984 event ($M_s = 6.2$) which was accompanied by a swarm of seismic activity, including 45 recorded shocks in the 3 months preceding the earthquake, and 10 aftershocks extending into 1986. Modeling of the main shock P and SH waveforms and a grid search fit to the body wave amplitudes indicates normal faulting along a NE–SW plane. Inversion of WWSSN P waveforms suggests a depth of 14 km and a source time function duration of 7 s; such figures preclude the anomalous low stress drops observed for documented volcanic earthquakes. We obtain similar focal mechanisms for the October 5 foreshock ($m_b = 5.5$) and the May 28, 1986 aftershock ($m_b = 5.5$). Relocation shows that the large June 30, 1945 earthquake (with Gutenberg magnitude $6\frac{3}{4}$) was an intraplate shock which occurred 400 km south of the 1984 epicentral region. Body waveform modeling and moment variance analysis of P, SH, Love, and Rayleigh waves suggest a normal faulting mechanism with east–west striking fault planes at a depth similar to the 1984 event. Small earthquakes also occurred near the 1945 epicenter in 1973, 1978, and 1985. The seismicity occurs in tectonically complex lithosphere formed just before a re-orientation of spreading on the Mathematicians Ridge associated with the elimination of offset along the Clarion Fracture Zone. SEASAT data indicate a significant gravity anomaly in the region of the 1945 event, which may represent a fracture zone of substantial offset, but no such features are found near the 1984 epicenter. The earthquakes suggest that concentrations of normal faulting intraplate earthquakes, found previously in the Indian Ocean; occur elsewhere in the oceanic lithosphere.

1. Introduction

It has long been recognized that continental intraplate earthquakes are preferentially located in certain active regions (e.g. the New Madrid and Charleston fault zones in North America). Thus, recent results showing that oceanic intraplate earthquakes are also located preferentially in various active zones are not necessarily surprising. As with continental earthquakes, it is not always easy to identify the cause of such concentrations of seismicity. In some cases, the seismicity is obviously linked to large-scale diffuse deformation; for example, the large intraplate earthquakes in the northern Indian Ocean (Stein and Okal, 1978; Bergman and Solomon, 1985; Wiens, 1986) are now interpreted as expressing a diffuse plate boundary (Wiens et al., 1985). However, other apparently isolated regions of activity are more puzzling, and not easily explained in terms of large-scale plate tectonics. Several such concentrations of seismicity have previously been identified along the Southeast Indian Ridge (Wiens and Stein, 1984; Bergman et al., 1984), at several locations in the South Pacific (Okal, 1984), and along the spreading centers near the Cocos plate (Wiens

0031-9201/87/$03.50

and Stein, 1984; Bergman and Solomon, 1984).

In this paper, we examine the seismicity of a region located ~ 600 km to the west of the Rivera Transform Fault (TF). This important offset of the East Pacific Rise separates the Pacific plate from the small Rivera plate to the north, while its eastern end forms the triple junction with the Cocos plate. As documented in detail by Mammareckx and Klitgord (1982), this is a region of complex tectonic history, which was involved in the reorientation of spreading at the time of the break-up of the Guadalupe plate (itself a remnant of the Farallon plate) ~ 12 Ma ago. More recently, an eastward ridge jump took place, leaving a dead rift known as the Mathematicians Ridge. As a result, available bathymetric and magnetic

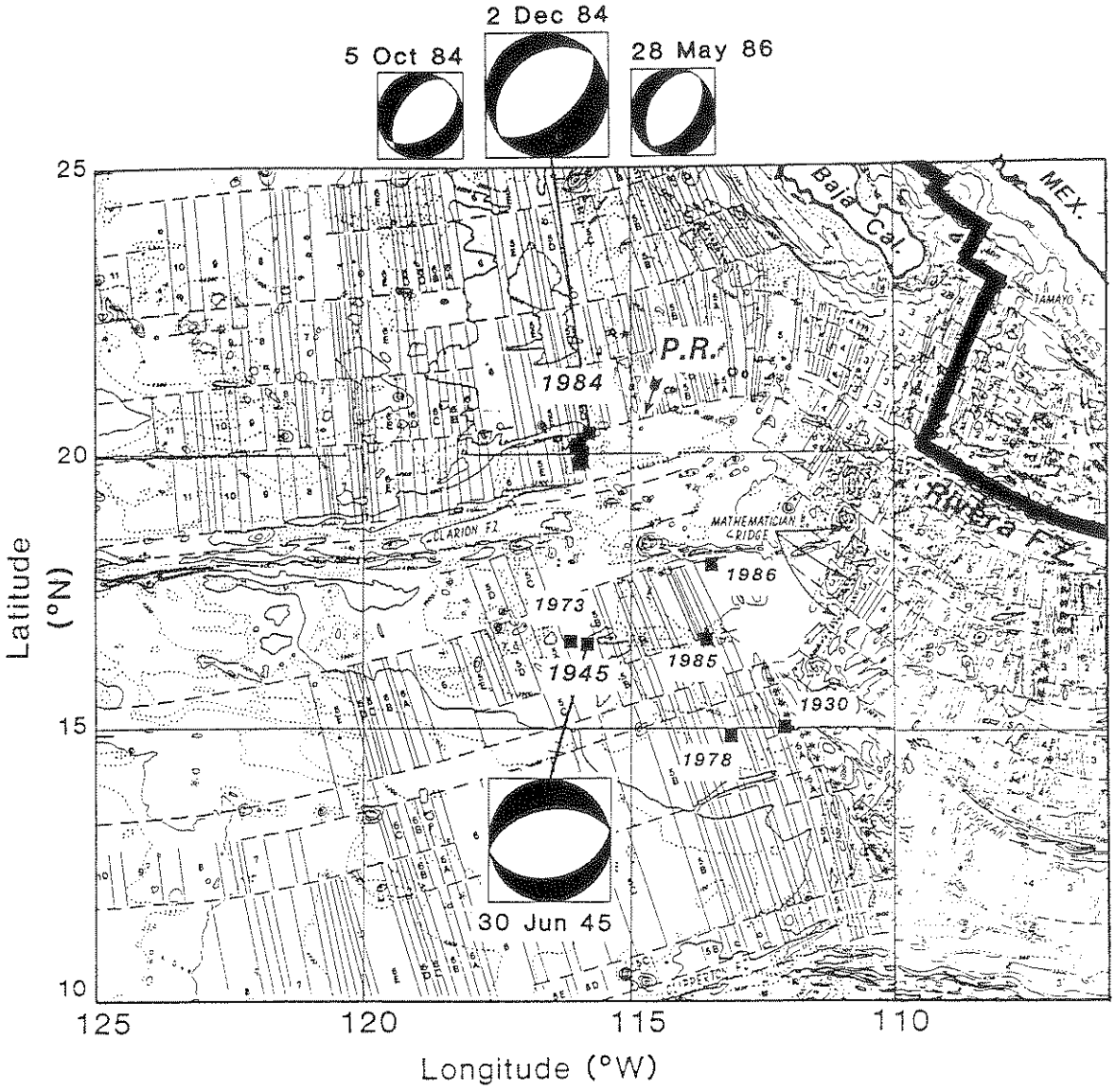

Fig. 1. Seismicity of the study area superimposed on bathymetry and magnetics from Klitgord and Mammerickx (1982). For the 1984 swarm, only events with $m_b >= 5.0$ have been plotted. 'P.R.' denotes Proto-Rivera Fracture Zone (see text). Focal mechanisms are those derived in this study. The boundary of the Pacific plate is shown as the thick line.

data in the region are particularly complex (Klitgord and Mammerickx, 1982).

The motivation behind the present study came from an extensive swarm of at least 54 earthquakes which took place in the area in 1984–1985, ~ 80 km north of the Clarion Fracture Zone (FZ), and 650 km southwest of the tip of Baja California (Fig. 1). The main shock on December 2, 1984 ($M_s = 6.2$) represents one of the largest oceanic intraplate events recorded in recent years. A compilation of historical seismicity shows that a major earthquake occurred ~ 400 km to the south on June 30, 1945 ($M = 6\frac{3}{4}$), together with smaller events in 1973, 1978 and 1985. These observations suggest that this part of the Eastcentral Pacific is a region of enhanced intraplate seismicity.

2. Seismological studies

2.1. The 1984–1985 Earthquake sequence

Between September 1984 and July 1985, 54 events were recorded near 20° N, 116° W in the Eastcentral Pacific. Figure 2 shows the time history of the swarm as reported by the Preliminary Determination of Epicenters (PDE) Bulletins. In addition, two events with magnitudes $m_b = 4.5$ and 5.5 occurred in April and May, 1986. Table I

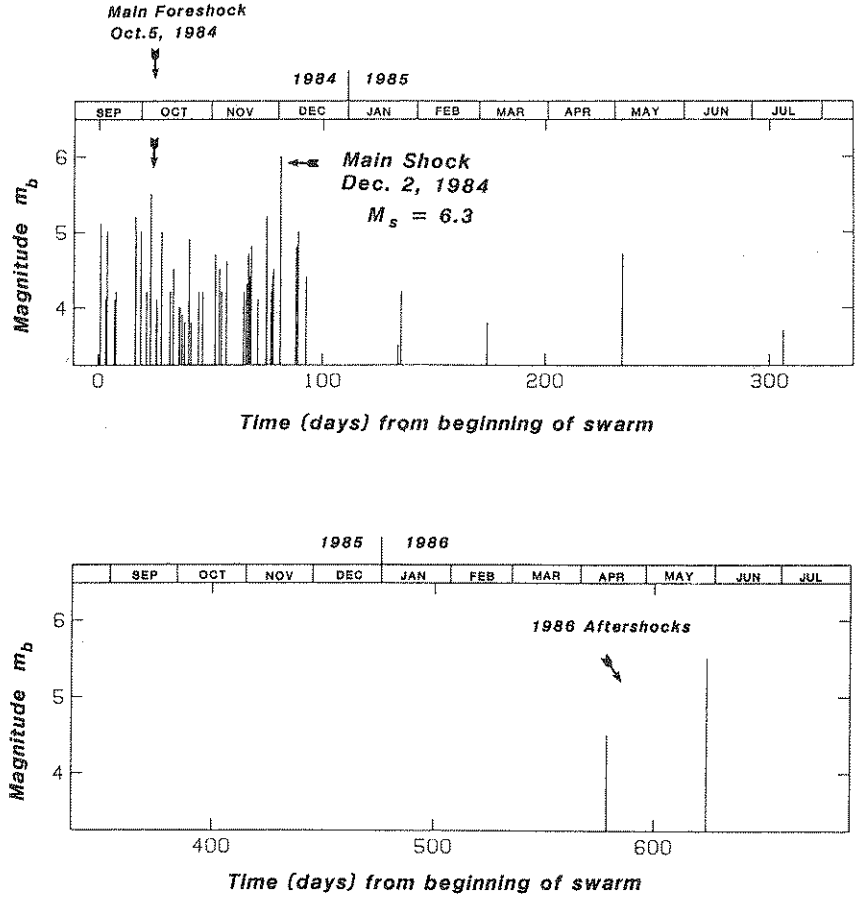

Fig. 2. (Top) Time history of the 1984–1985 swarm derived from the monthly listings of the Preliminary Determination of Epicenters. Before September 1984 no seismicity had been detected in the immediate epicentral region . (Bottom) Continuation to 1986. Note apparent end of swarm, period of quiescence, followed by the two 1986 aftershocks.

TABLE I

Epicentral parameters of the 1984–1985 swarm

Date Year	Month	Day	Origin time GMT	Latitude °N	Longitude °W	Number of stations	Magnitudes m_b	Magnitudes M_s
1984	09	12	21:56:27.1	19.87	115.89	85	5.1	4.6
1984	09	15	05:46:57.3	20.13	115.75	11	4.1	
1984	09	15	19:52:02.3	20.09	115.89	75	5.0	4.1
1984	09	19	06:40:47.6	20.23	115.37	17	4.1	
1984	09	19	20:55:22.1	19.10	115.87	23	4.2	
1984	09	28	12:07:41.8	20.11	115.93	87	5.2	5.1
1984	09	28	15:42:01.1	20.07	115.87	72	5.0	4.0
1984	10	01	00:23:12.5	19.86	115.88	80	5.0	
1984	10	03	12:13:56.7	19.46	115.94	19	4.2	
1984	10	05	06:23:31.8	20.02	115.78	21	4.5	3.4
1984	10	05	09:48:44.3	20.10	116.01	126	5.5	4.6
1984	10	07	23:20:37.6	20.19	115.70	15	4.1	3.2
1984	10	08	04:15:18.7	20.14	115.77	18	4.0	
1984	10	10	02:19:21.2	19.83	115.96	50	5.0	4.0
1984	10	13	23:05:12.0	19.89	116.08	12	4.2	
1984	10	15	10:23:04.0	19.62	116.09	31	4.5	
1984	10	17	22:33:44.9	19.47	115.68	9	4.0	3.7
1984	10	18	07:19:18.3	19.95	115.84	15	4.0	
1984	10	19	07:23:22.3	19.61	116.10	7	3.9	
1984	10	20	10:19:13.4	20.11	115.86	15	3.8	
1984	10	22	07:59:34.4	20.01	115.94	67	4.9	4.1
1984	10	23	07:26:52.5	20.52	115.54	9	3.8	3.2
1984	10	26	16:32:26.2	19.52	116.14	15	4.2	4.1
1984	10	28	12:33:52.7	20.20	115.67	6	4.2	3.0
1984	11	03	03:01:39.1	20.18	116.02	33	4.7	4.0
1984	11	04	21:49:31.5	20.24	115.70	26	4.5	3.9
1984	11	05	21:11:03.3	20.13	115.76	13	4.2	
1984	11	08	02:17:31.0	20.13	115.94	16	4.6	
1984	11	15	20:24:18.7	20.04	115.74	17	4.2	
1984	11	17	00:17:40.3	20.29	115.70	14	4.1	
1984	11	17	04:38:02.4	20.05	115.78	21	4.3	
1984	11	17	20:58:02.3	20.12	115.89	34	4.7	
1984	11	18	12:20:54.7	20.14	115.62	18	4.4	
1984	11	19	04:54:48.0	20.21	115.94	28	4.8	
1984	11	22	06:41:39.9	20.02	115.69	14	4.1	
1084	11	26	01:12:33.1	20.24	115.89	105	5.2	4.6
1984	11	26	05:07:54.7	20.18	115.83	25	4.6	3.7
1984	11	26	07:16:07.3	20.08	115.41	7	4.2	3.9
1984	11	28	03:51:38.4	19.81	115.97	15	4.2	
1984	11	28	17:51:05.6	19.64	115.93	17	4.4	
1984	11	28	20:19:39.1	19.79	115.76	6	4.2	
1984	11	28	22:11:03.3	19.91	115.74	6	3.6	
1984	11	28	23:44:31.1	20.11	116.03	20	4.4	
1984	11	29	06:02:44.8	20.13	115.80	24	4.5	3.3
1984	12	02	05:34:13.7	19.77	115.94	14	4.4	
1984	12	02	06:09:44.0	20.36	115.76	264	6.0	6.2
1984	12	02	08:19:56.7	20.01	115.73	20	4.4	
1984	12	09	06:52:38.1	20.08	115.81	53	4.8	4.3
1984	12	10	03:31:56.6	20.17	115.99	96	5.0	4.4
1984	12	13	18:23:30.5	20.17	115.76	13	4.4	3.3
1985	01	23	20:36:21.7	20.54	115.66	7	3.5	
1985	01	25	06:21:43.6	19.86	115.90	12	4.2	
1985	03	04	19:33:44.7	19.56	115.27	7	3.8	
1985	07	14	21:43:26.7	20.39	115.56	19	3.7	3.3
1986	04	13	09:57:02.0	20.11	115.99	21	4.5	
1986	05	28	13:33:44.1	19.98	115.93	105	5.5	5.1

is a complete listing of the location parameters for all events detected in the region, as of February 6, 1987. The 48 foreshocks occurred at an approximately uniform rate between September 12, when the swarm commenced with an $m_b = 5.1$ event, and December 2, when the $M_s = 6.2$ main shock occurred. Despite the overall uniform rate of activity, short periods of quiescence occurred between September 19 and 28 and between November 8 and 15. A large number of small events, preceded by an $m_b = 5.2$ shock, were recorded on November 26–29, followed by 3 days of quiescence before the main shock. A small event ($m_b = 4.4$) preceded the main shock by ~ 30 min. Only 10 aftershocks were recorded; predominance of foreshocks over aftershocks is strong indication of the swarm-like nature of the sequence.

On the other hand, the 1984 swarm does not show the anomalous frequency–magnitude relationship often found in swarms (Fig. 3). Its b value, calculated using the maximum likelihood formulation of Aki (1965) for a minimum magnitude of 4.2, is 1.05, with 90% confidence limits of ± 0.26. Successive calculations showed that the b value exhibits little variation for different assumed minimum values down to 4.2, indicating nearly uniform detection above that magnitude. The b value of 1.05 lies close to the global average of 0.9

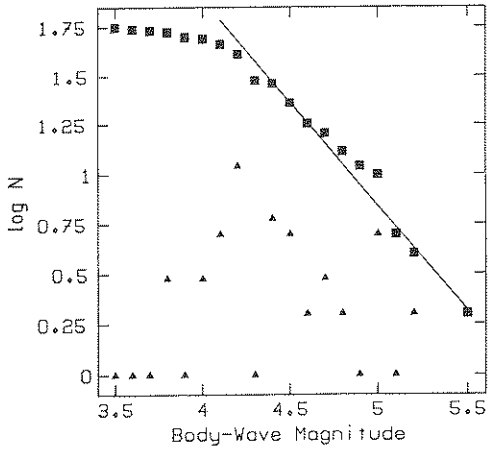

Fig. 3. Frequency–magnitude characteristics of the swarm. Solid squares denote cumulative frequency, triangles the number of earthquakes within each m_b window of 0.1 unit. The solid line corresponds to the maximum likelihood b value slope of 1.05.

for oceanic intraplate earthquakes reported by Bergman and Solomon (1980). It is significantly lower than that derived from other oceanic swarms such as those on the Mid-Atlantic Ridge ($b = 1.3$) (Sykes, 1970), the 1968 Fernandina Caldera collapse ($b = 1.24$–2.53) (Francis, 1974), and the Gilbert Islands swarm of 1981–1983 ($b = 1.35$) (Lay and Okal, 1983). This difference in character is not surprising, if only since the latter swarms did not feature a clear 'main shock'.

Figure 4a shows the geographic distribution of all swarm events. The north–south region defined by the entire epicentral dataset is probably an artifact of the station distribution: for the smaller events detected only by North American stations, resolution becomes poor, and the uncertainty ellipses elongated, in this direction. More significantly, the larger and better-located events ($m_b \geq 5.2$; see Fig. 4b) are concentrated along a 30 km long zone oriented NE–SW, which we will show, coincides with the fault plane orientations found from our body wave studies. The two aftershocks which occurred in 1986 were located 30 km to the south of this line, a distance significantly larger than the uncertainty in the location of the largest one.

2.2. The June 30, 1945 earthquake

The June 30, 1945 event, which occurred ~ 400 km south of the 1984–1985 sequence, was well recorded by a large number of stations in the Americas and Europe, as well as in Hawaii and New Zealand. As a result, the precision of its relocation is particularly good, given the magnitude and date of the earthquake. P wave arrival times listed in the International Seismological Summary (ISS) were used in an iterative least-squares relocation program, eliminating arrival times which show a residual of more than 2.5 times the root mean square (rms) residual between iterations. On the basis of the body wave modeling (see below), we fixed the hypocentral depth at 12 km.

The final solution, based on arrival times from 55 stations, gave latitude 16.6° N, longitude 115.8° W, with an rms residual of 2.0 s. This location is ~ 1° SW of that given by Gutenberg

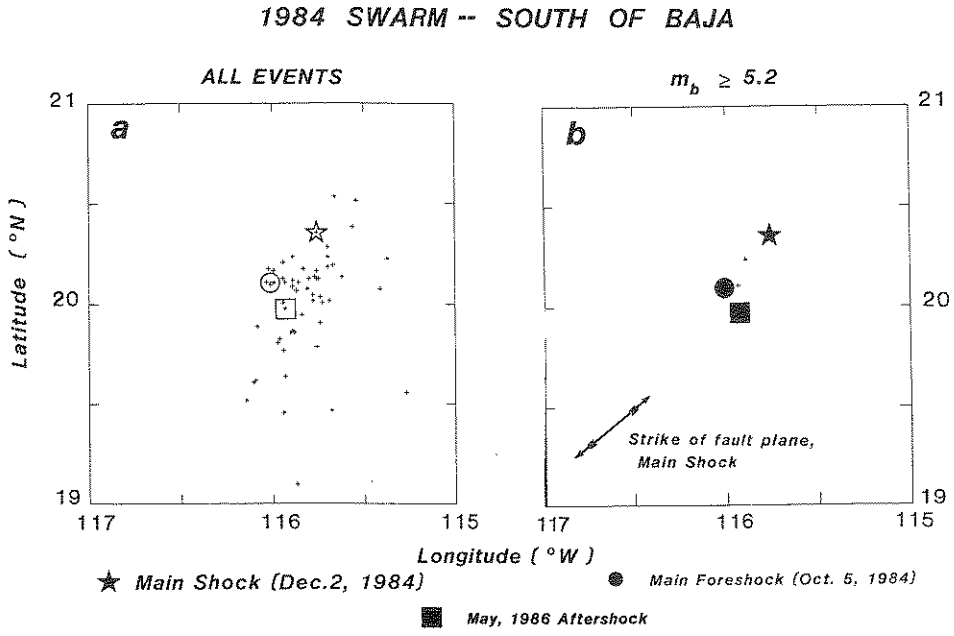

Fig. 4. Geographic distribution of the swarm events, as located in the PDE listings. (Left) All events scatter over a considerable area with a north–south trend, probably due to the orientation of the uncertainty ellipse associated with a typical station distribution. (Right) Well located events ($m_b = 5.2$) define a much smaller region and are apparently aligned with the main shock nodal planes.

and Richter (1954) (17°N, 115°W). The 90% confidence ellipse, calculated using the procedure of Flinn (1965), suggested uncertainties in latitude and longitude of ±0.2°. As the nearest plate boundary, the Rivera Fracture Zone, is ~ 750 km away, this relocation firmly establishes the intraplate nature of the event.

2.3. Other events

We systematically searched the NOAA tape of epicenters for all instrumental intraplate seismicity in the area located between latitudes 10 and 25°N, and longitudes 135 and 105°W, for the years 1900–1983, to detect any possible extension

TABLE II

Other seismic events in the study area

Date Year	Month	Day	Origin time GMT	Latitude (°N)	Longitude (°W)	Number of stations	rms residual (s)	Magnitudes m_b	Magnitudes M_s
Confirmed									
1945	06	30	05:31:20	16.6	115.8	55	2.0		$6\frac{3}{4}$
1973	05	07	16:27:13.1	16.65	116.12	77		4.7	
1978	08	27	01:10:28.4	14.93	113.07	40		5.0	5.2
1985	05	04	12:47:09.9	16.67	113.53	67		4.7	4.5
1986	03	24	19:43:23.4	18.01	113.44	37		5.0	5.7
Tentative									
1930	09	22	05:01:47	15.08	112.07	6	3.0		

TABLE III

Other intraplate epicenters in the Eastcentral Pacific

Date Year	Month	Day	Origin time GMT	Latitude (°N)	Longitude (°W)	Number of stations	rms residual (s)	Magnitudes m_b	Magnitudes M_s
Confirmed									
1949	12	10	19:15:45	4.12	128.85	17	1.7		$5\frac{3}{4}$
1961	07	23	14:37:53	6.81	123.67	20	1.5		$5\frac{7}{8}$
1963	10	06	08:48:12.4	21.9	127.4	13		4.0	
1966	09	24	08:57:10.2	12.0	130.8	38		5.2	
1977	08	04	11:06:52.2	2.530	115.747	28		4.6	
1983	06	12	18:30:06.5	4.654	112.061	8		4.6	4.3
1983	06	25	02:46:39.8	10.530	130.324	21		4.6	4.3
Tentative									
1933	01	04	21:10:45	28.42	126.99	17	2.2		6.0

of the seismic activity outside of the immediate vicinity of the earthquakes studied. We eliminated from the results all events related to the East Pacific plate boundary, as well as a series of earthquakes along the southern tip of the Baja peninsula, which probably have their origin in a localized stress field. * Because of the fundamentally different epicentral accuracies involved, we discuss separately the resulting datasets before and after 1963.

For the period postdating 1963, Table II shows that several small recent events have occurred in the general region of the 1945 earthquake. An $m_b = 4.7$ event occurred in 1973 within 40 km of the 1945 epicenter, suggesting a possible reactivation of the same fault. Three events with $m_b = 4.7$–5.0 also occurred east of the 1945 epicenter in 1978, 1985 and 1986 (Fig. 1). The remainder of the study area has been extremely quiet since 1963, with only five events scattered over more than 4×10^6 km^2.

The situation is much more uncertain regarding the historical (pre-1963) earthquakes. In addition to the 1945 event, our computer search of the NOAA tape initially suggested 35 events. Among those, eight were not listed in the ISS, 12 were listed but with too few data, six relocations failed to converge to a solution stable with respect to a restriction of the dataset, and five relocated to the plate boundaries. Among the four new intraplate solutions found, two achieved rms residuals of 2 s or less with a considerable number of arrival times, giving these locations a degree of confidence comparable to present-day locations. We report them as 'confirmed' locations in Tables II and III. The remaining two relocations had generally fewer reported arrivals and rms residuals of between 2 and 3.5 s; past results suggest that these locations may be in error by several degrees (Stein et al., 1987). We label these two relocations (in 1930 and 1933) as 'tentative' in Tables II and III.

The picture emerging from this compilation is the following:

(1) the 1984–1985 swarm and its 1986 aftershocks make up an isolated cluster of seismicity;

(2) two events (in 1973 and 1985) are aligned with the 1945 shock along an east–west line, which we will see coincides with the strike of the fault plane;

(3) a diffuse patch of seismicity comprising four events exists along the Mathematicians Ridge and its western slope (1978, 1985, 1986, and possibly 1930); and

(4) the rest of the Eastcentral Pacific is an extremely quiet seismic zone.

It should be noted that we have taken the

* We also eliminated 12 or so Philippine earthquakes erroneously given on the NOAA tape a Western, rather than Eastern, longitude of between 120 and 130°. While these errors are obvious when confronted with ISS listings, they stress the extreme caution to be used when interpreting historical events from a single source such as the NOAA tape.

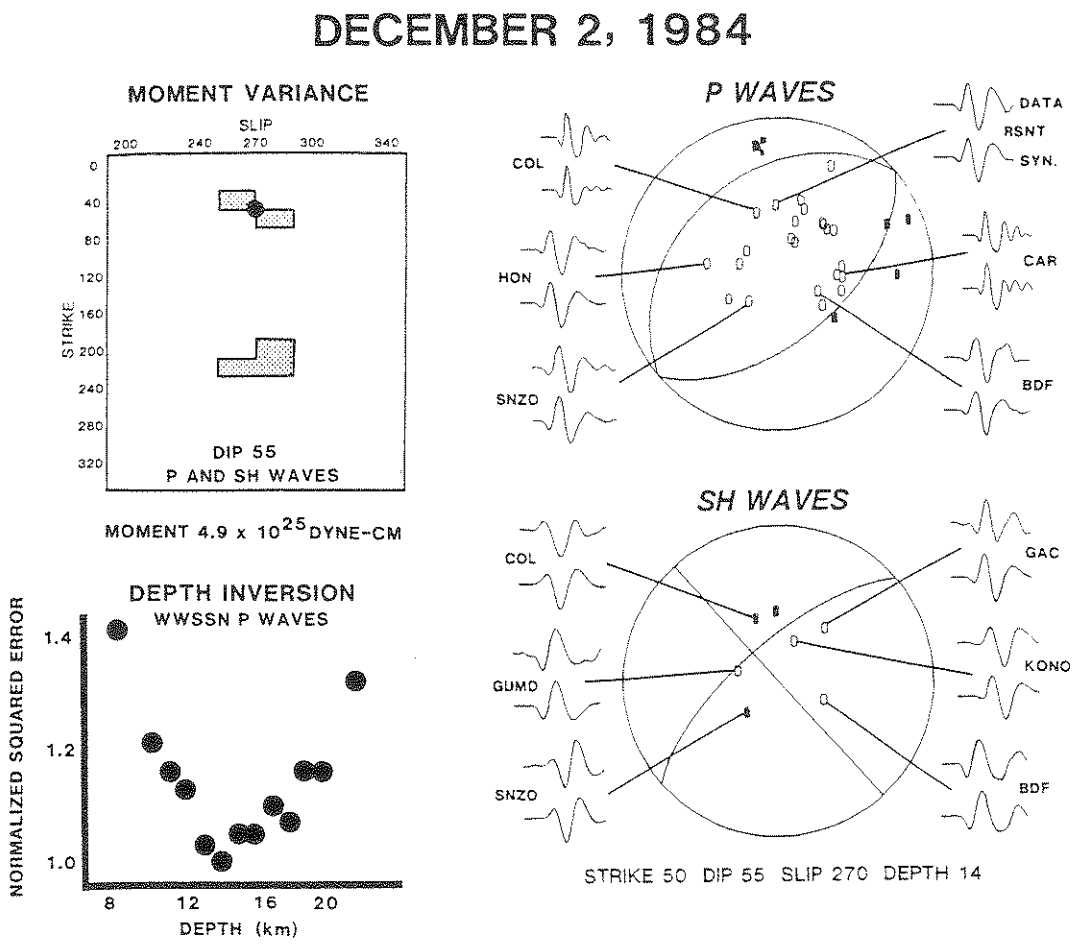

Fig. 5. Mechanism determination for the December 2, 1984 mainshock. (Upper left) Grid search for the mechanism best fitting the polarities and P and SH amplitudes for a dip of 55°; grid searches for other dips showed higher errors. (Right) P and SH focal mechanisms, with some waveforms, along with synthetic seismograms computed for the chosen mechanism and depth and a total time function duration of 7 s. SH polarity follows Kanamori and Stewart's (1976) convention. (Lower left) Normalized squared error as function of focal depths for WWSSN P waves, indicating a depth of 14 km.

conservative approach of deleting all historical events for which relocation results were too poor to ensure an intraplate character; however, we cannot, in several occasions, affirm that those earthquakes are interplate; therefore, there remains the possibility of additional small historical intraplate earthquakes in the area.

2.4. *Focal mechanisms*

Three events from the 1984–1985 swarm proved large enough for a study of their mechanism: the December 2, 1984 mainshock ($m_b = 6.0$; $M_s = 6.2$), the largest foreshock on October 5, 1984 ($m_b = 5.6$; $M_s = 4.6$), and the May 28, 1986 aftershock ($m_b = 5.5$; $M_s = 5.1$). Figure 5 shows the mechanism determination for the mainshock; P and SH first motions from GDSN stations and several stations in California and Mexico provide tight constraints and suggest a normal faulting mechanism with nodal planes oriented northeast–southwest. Study of P and SH waves from GDSN stations using standard body wave modeling techniques (e.g. Langston and Helmberger, 1975) fur-

ther constrain the mechanism and provide a good fit to the data. In addition to fitting the waveforms, we used a grid-search technique to determine the solution best fitting the P and SH amplitudes by finding the mechanism which produced the least variance between moments determined from different waveforms (Fig. 5, top left). The seismic moment, 4.9×10^{25} dyn-cm, suggests that this is one of the largest recent oceanic intraplate earthquakes.

To constrain the depth and source time function of the event, and because the long-period nature of the GDSN instrument response limits the resolution of these parameters, we also inverted the P waveforms from seven azimuthally distributed WWSSN stations. The inversion consists of deconvolving the suite of seismograms using a variation of Kikuchi and Kanamori's (1982) algorithm, and kernels generated for several depths. The best-fitting centroid depth and source time function are obtained as those minimizing the deconvolution error. Tests with synthetics (Stein and Wiens, 1986) have shown that this is a robust method for determining depth and time function, even in the presence of source complexity or small errors in mechanism. Since this method determines the depth without a priori assumptions on the source time duration, it helps resolve the partial trade-off often found between these parameters for shallow earthquakes (Wiens, 1985).

Figure 5 shows some waveforms and synthetics, as well as a plot of error vs. depth for WWSSN P waves. The centroid depth indicated by the error minimum is 14 km; we estimate the uncertainty as ± 2 km. The deconvolution indicates a simple source time function of 7 s duration. We also examined possible trade-offs between depth and focal mechanism parameters by inverting the data with other possible mechanisms, and found this depth to be robust with respect to small changes in mechanism parameters.

As the source time function provides information on the extent of the rupture, we can put constraints on the stress drop $\Delta\sigma$ from the formula

$$\Delta\sigma = C\frac{M_0}{LW^2} \tag{1}$$

where C is a constant depending on the fault geometry and Poisson ratio of the material (~ 1 in most common cases), M_0 is the seismic moment, and L and W are the length and width of a rectangular fault (Kanamori and Anderson, 1975). Both the source time function (assuming a rise time of 1 s, and a rupture velocity of 0.8 times the shear velocity) and the extent of the swarm's epicentral area (restricted to well-located earthquakes; $m_b \leq 5.2$) suggest a maximum fault length $L \simeq 45$ km. The width of the fault is limited by the extent of the brittle zone for oceanic lithosphere this age, giving $W \leq 20$ km. Thus, a minimum value $\Delta\sigma = 25$ bar is obtained. Very low stress drops, such as those observed during volcanic events such as the Fernandina caldera collapse (1 bar, Kaufman and Burdick (1980)), would require either unrealistic fault lengths, or fault widths extending deep into the ductile zone of the mantle, or both. In brief, this earthquake does not exhibit anomalously low stress drop.

The dataset for the October 5 foreshock was much more limited, since the signal was near the noise level at many GDSN stations, and no clear first motions were observed for stations outside North America. Figure 6 shows the mechanism determined for the October 5 event, along with observed and synthetic body waves. The procedure was the same as for the December 2 event, using waveform modeling and a grid-search fit to the P and SH amplitudes. The poor station-distribution for this event resulted in greater uncertainties in the mechanism. The fault strike has particularly large uncertainties, acceptable strikes range from $\sim$N30°E to N90°E, but the best fitting solution is basically that of the December 2 event. The waveforms were best fit by a model depth of 13 km (with fairly large uncertainties resulting from the long period nature of the GDSN instrument response) and a moment of 1.4×10^{24} dyn-cm. Figure 7 similarly shows results for the May 28, 1986 aftershock. The focal parameters obtained are, again, very similar to those of the main shock.

Results recently obtained by an automated moment tensor inversion of long period body waves (Dziewonski et al., 1985) are in general agreement with the focal mechanisms determined in this study. The Harvard mechanism for the main shock

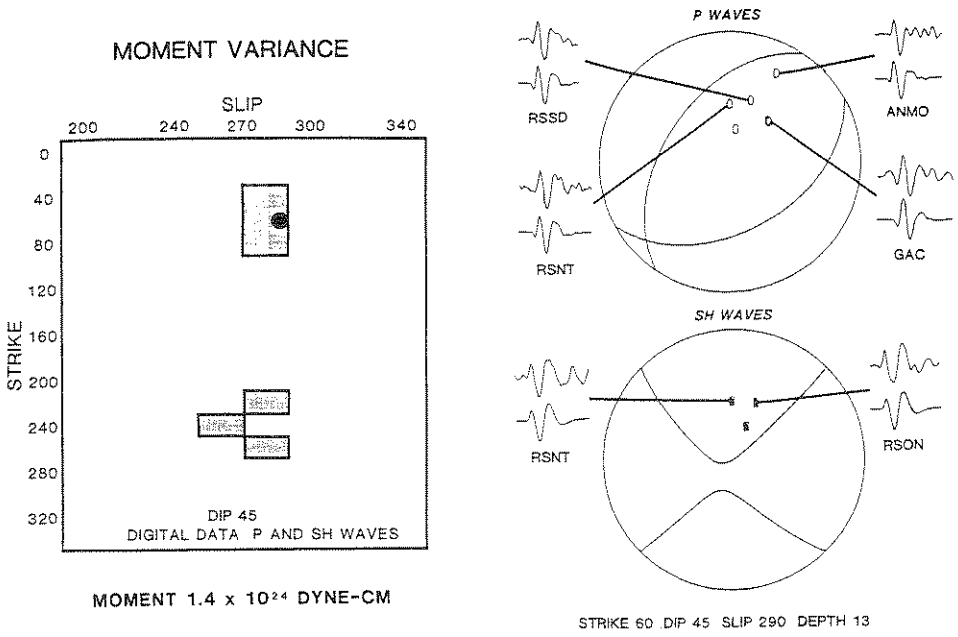

Fig. 6. Mechanism determination for the October 5, 1984 foreshock. Methodology follows that of the main shock (see caption to Fig. 5). Poor station-distribution results in larger uncertainties.

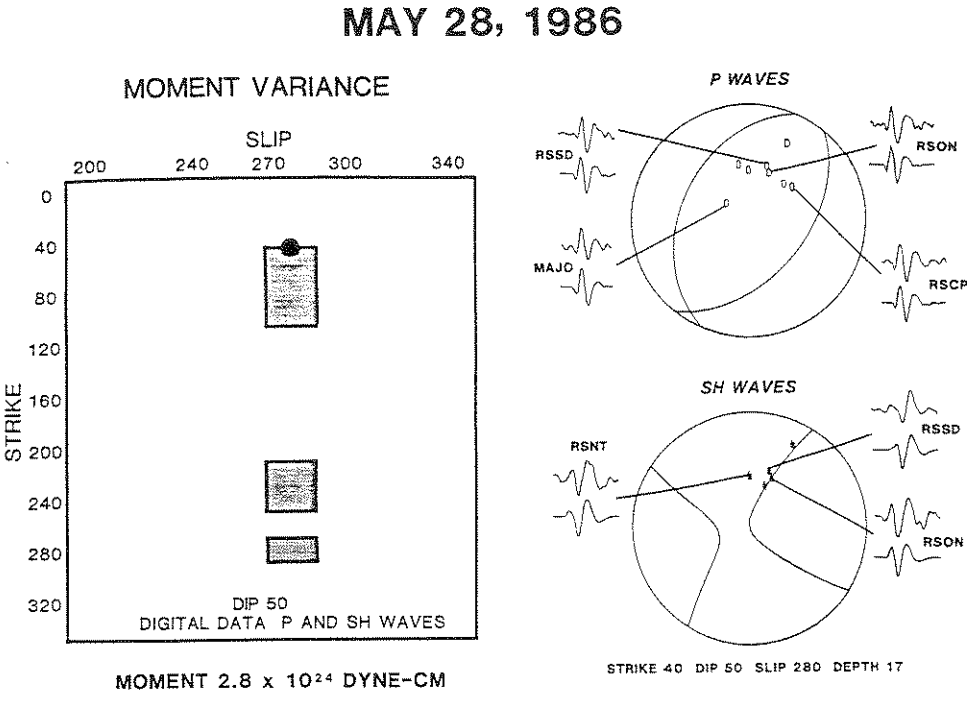

Fig. 7. Same as Fig. 6 for the May 28, 1986 aftershock.

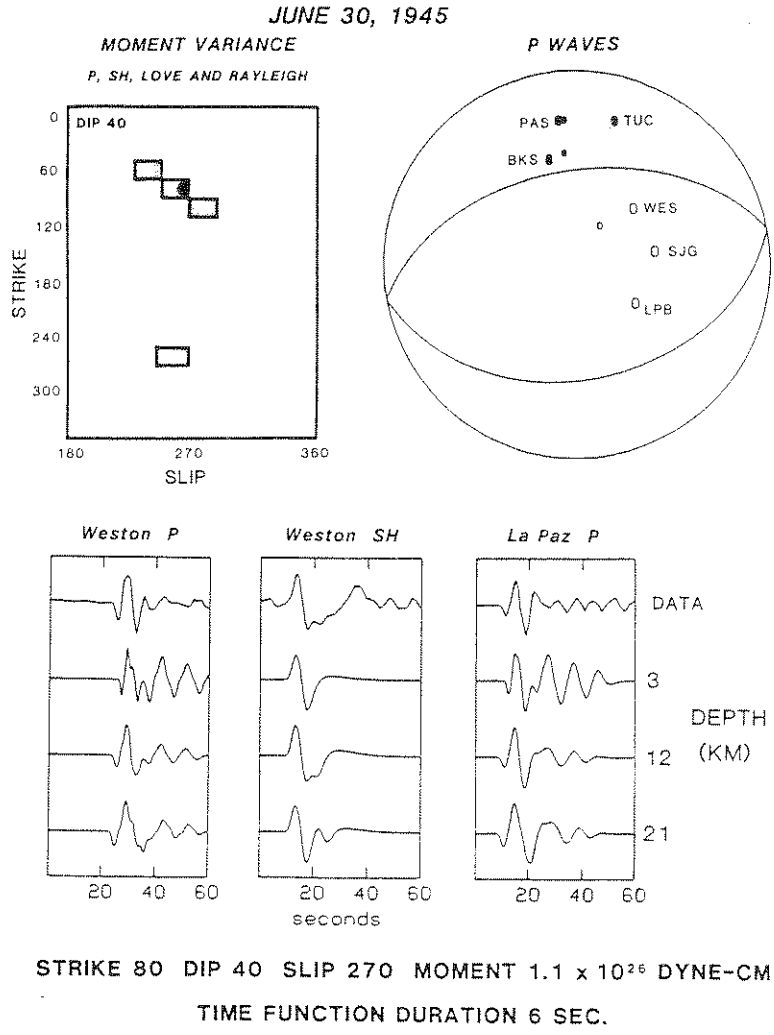

Fig. 8. Mechanism determination for the June 30, 1945 earthquake. (Top left) Moment variance results giving the mechanism best fitting the polarities and P, SH, Love, and Rayleigh wave amplitudes (Wiens, 1986). Dips other than 40° showed higher errors. (Top right) Inferred P wave focal mechanism. Large symbols denote distinct impulsive first motions from actual records, small symbols show polarities reported to the ISS. (Bottom) Body wave modeling for the 1945 event. The synthetics provide a good fit to the data at a depth of 12 km with a total time function duration of 6 s.

(strike = 42°, dip = 66°, slip = 268°) has a steeper dip for the southeast dipping nodal plane. The mechanism determined here provides a better fit to several of the SH waveforms, to P wave dilatations recorded in South America, and to the strong compressional P wave first motion recorded at Pasadena. The Harvard solution for the October 5 foreshock (strike = 83°; dip = 61°; slip = 282°) and the May 28, 1986 aftershock (strike = 53°; dip = 64°; slip = 271°) are also consistent with ours.

Figure 8 shows the focal mechanism determination for the June 30, 1945 event. Impulsive P wave first motions from western U.S. stations indicate compression, whereas P waves from Weston, San Juan, and La Paz indicate dilatation. However, the P wave first motions alone are insufficient to determine a unique focal mechanism.

To refine our solution, we used the moment variance technique, as introduced by Wiens (1986). This is a particularly robust method for obtaining

focal mechanisms from sparse data sets. It determines a focal mechanism through a grid search analysis optimizing the fit to a dataset which may include P wave first motions, P, SH, Love, and Rayleigh amplitudes, and S wave polarizations. The advantage of this method is that it uses a large number of constraints simultaneously to determine the best fitting mechanism, thus minimizing the reliance on an individual datum; it also allows the model space to be examined for local minima, which may be a problem with sparse data sets. Tests with data from recent earthquakes of known mechanism show that this procedure can accurately determine focal mechanisms given data from as few as one or two stations (Wiens, 1986).

Figure 8 (top left) shows the moment variance results using P waves from La Paz and Weston, SH waves from Weston, and Love and Rayleigh waves from Weston, Pasadena, and Christchurch. The figure represents a slice through the model space at a constant dip of 40° with minima in moment variance outlined. Both minima represent normal faulting on east–west trending planes. Similar analyses were performed with other dips; they resulted in higher errors. The best fit to the amplitudes was achieved for the focal mechanism shown in Fig. 8.

The normal faulting mechanisms provided an excellent fit to the body waves, as shown in Fig. 8 (bottom). The body waveforms are well matched by models generated for a depth of 12 km, and a simple trapezoidal time function with a duration of 6 s. The median moment obtained from the body and surface wave analysis is 1.1×10^{26} dyn-cm.

The 1973 and 1978 events in the immediate vicinity of the 1945 epicenter were too small to produce identifiable long period body waves, and we could not find enough clear short period P wave first motions to justify an attempt at focal mechanism determination. However, the small number of distinct first motions available are consistent with normal faulting mechanisms. Source parameters obtained in this study are summarized in Table IV.

3. Local tectonics and SEASAT data

3.1. Tectonic context

In this section, we discuss the general tectonic framework of the epicentral areas. We base our study on the detailed tectonic reconstruction and maps by Klitgord and Mammerickx (1982) and Mammerickx and Klitgord (1982). Figure 1 is adapted from these authors' plates, and correlates the epicenters with their data. In addition, we use SEASAT altimetry data, to investigate the geoid signature of a number of local features in the area. SEASAT coverage of the area is shown in Fig. 9.

As mentioned earlier, this part of the Pacific Ocean floor has undergone a number of complex spreading reorientations and ridge jumps since the Mid-Miocene. In particular, the oceanic lithosphere in the epicentral area of the 1984–1985 swarm was produced just before the change in spreading direction along the Mathematicians Ridge from NNW–SSE to WNW–ESE at about 12 Ma (Mammerickx and Klitgord, 1982).

A major tectonic feature in the area is the

TABLE IV

Source parameters determined in this study

Date			Focal mechanism							Depth (km)	Seismic moment (10^{25} dyn-cm)
Year	Month	Day	Strike (°)	Dip (°)	Slip (°)	P Axis		T Axis			
						Plunge (°)	Azimuth (°)	Plunge (°)	Azimuth (°)		
1945	06	30	80	40	270	85	170	5	350	12±4	11.0
1984	10	05	60	45	290	76	53	2	316	13±5	0.14
1984	12	02	50	55	270	80	320	10	140	14±2	4.9
1986	05	28	40	50	280	81	3	5	123	15±5	0.28

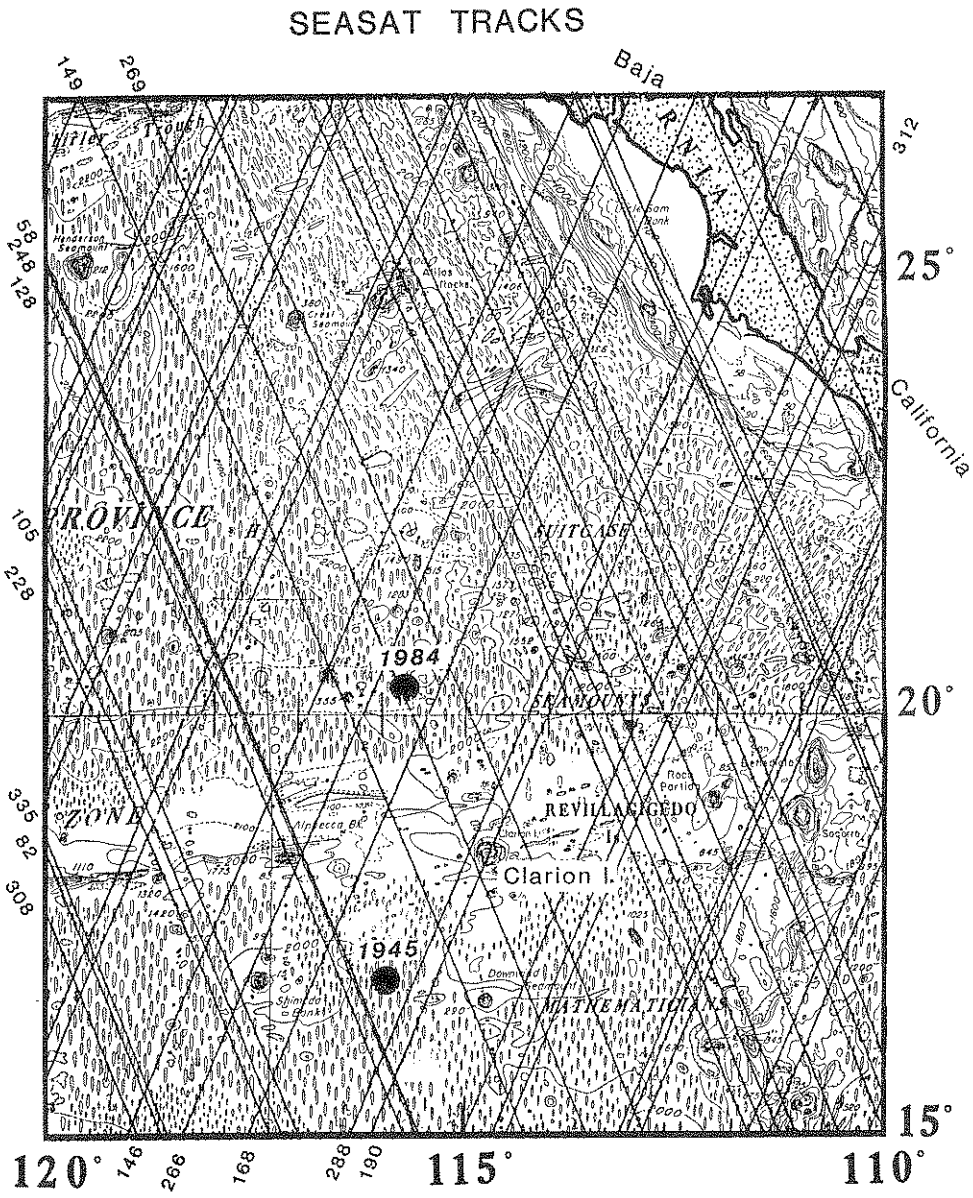

Fig. 9. SEASAT coverage of the area under study, superimposed on bathymetry by Chase et al. (1970). The large dots are the epicenters of the 1945 and 1984 events.

Clarion Fracture Zone, well identified in the bathymetry and magnetics from our study area all the way to the Line Islands (165° W). In our region of interest, it features a South to North drop in the geoid of 60 cm (see Fig. 10). According to various models of the thermomechanical evolution of the lithosphere (e.g. Cazenave and Okal, 1986), and for an ocean floor on the average 12 Ma in age, this offset corresponds to an age gap of 6 Ma between the two sides of the FZ, in agreement with the magnetic anomaly offset mapped by Klitgord and Mammerickx (1982) (e.g. 5c and 6 at 117° W). Further east, both the bathymetric expression and the SEASAT signature of

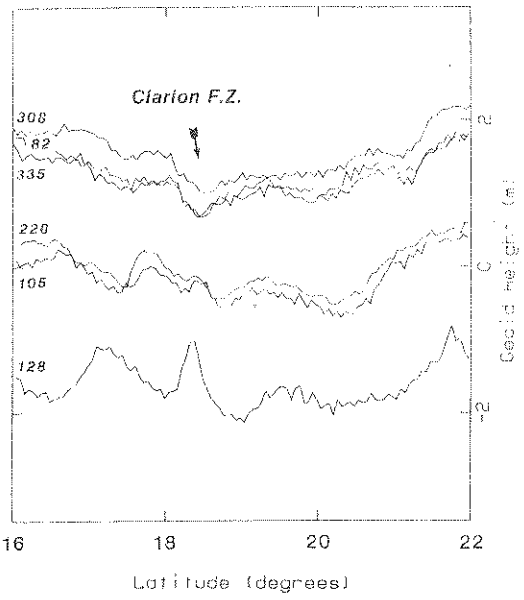

Fig. 10. Residual geoid height along selected ascending SEASAT tracks across the Clarion FZ. Note disappearance of signal East of 116° W. Linear trend over range of latitudes plotted has been subtracted from data. Each track is offset linearly in longitude.

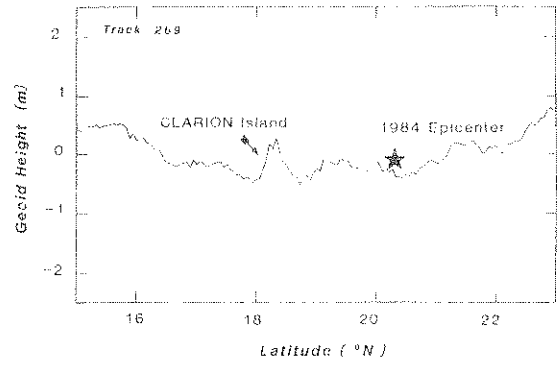

Fig. 11. Residual geoid height along SEASAT track 269, passing over 1984 epicenter. Note absence of significant signal. Linear trend over range of latitudes plotted has been subtracted from data.

the Clarion FZ die out around 116° W. This rapid decrease in age offset around the time of anomaly 5 was related to the transfer of spreading from the Farallon system to the Mathematicians Ridge.

The 1984 epicenter falls 80 km north of the Clarion system, in the immediate vicinity of a smaller fracture zone identified in the magnetic record by Klitgord and Mammerickx (1982) continuously from 117° W eastward. These authors map it as continuous with the southern boundary of the Rivera Fracture Zone. West of 117° W, this 'Proto-Rivera' FZ is offset a few kilometers to the North. Its age offset, ~ +1 Ma to the North in the epicentral area, changes polarity (to +1 Ma to the South) west of 120° W. Thus, the Proto-Rivera FZ behaved as a minor 'zero-offset-transform' during the Miocene, and may have controlled the process of stabilization of the Rivera TF at its present location. While it could be tempting to interpret this feature as a zone of weakness responsible for preferential stress release, we must keep in mind that its offset (1 Ma) would create a bathymetric signature of < 100 m and a geoid signal of ~ 10 cm, both of which would go undetected with present technology. It is indeed doubtful whether bathymetric accidents on such a small scale are the exception or the norm on the ocean floor. In any case, the geoid signature along track 269 passing exactly above the 1984 epicenter reveals no anomalous signal (Fig. 11).

In the area of the 1945 shock, Mammerickx and Klitgord's (1982) reconstruction shows lithosphere approximately the age of anomaly 5b (15 Ma), having been generated at the Pacific–Guadalupe Ridge. As shown in Fig. 12, seven SEASAT tracks consistently reveal a prominent step-like feature at ~ 16.8° N. Its geoid signature on tracks 128, 248, 58, 149, 168, 288 and 190 is typical of a fracture zone, and we tentatively interpret it as a short 'Downwind–Shimada' FZ, which we name after two bathymetric features which grossly delineate its extension (the Downwind Seamount and the Shimada Bank). Its polarity is down (older) to the South; its offset Δh in the geoid is 70 cm, which would correspond to an age offset Δa of 6.5 Ma, using an average $\Delta h/\Delta a = 10.5$ cm a^{-1} (Cazenave and Okal, 1986). The Downwind–Shimada FZ is recognized from 118 to 114.5° W, indicating that it was active along the Pacific–Guadalupe Ridge only from 19 Ma to the reorganization at the Mathematicians Ridge at 12 Ma. Possibly because of this short period of activity, it is not mapped in Klitgord and Mammerickx's (1982) study.

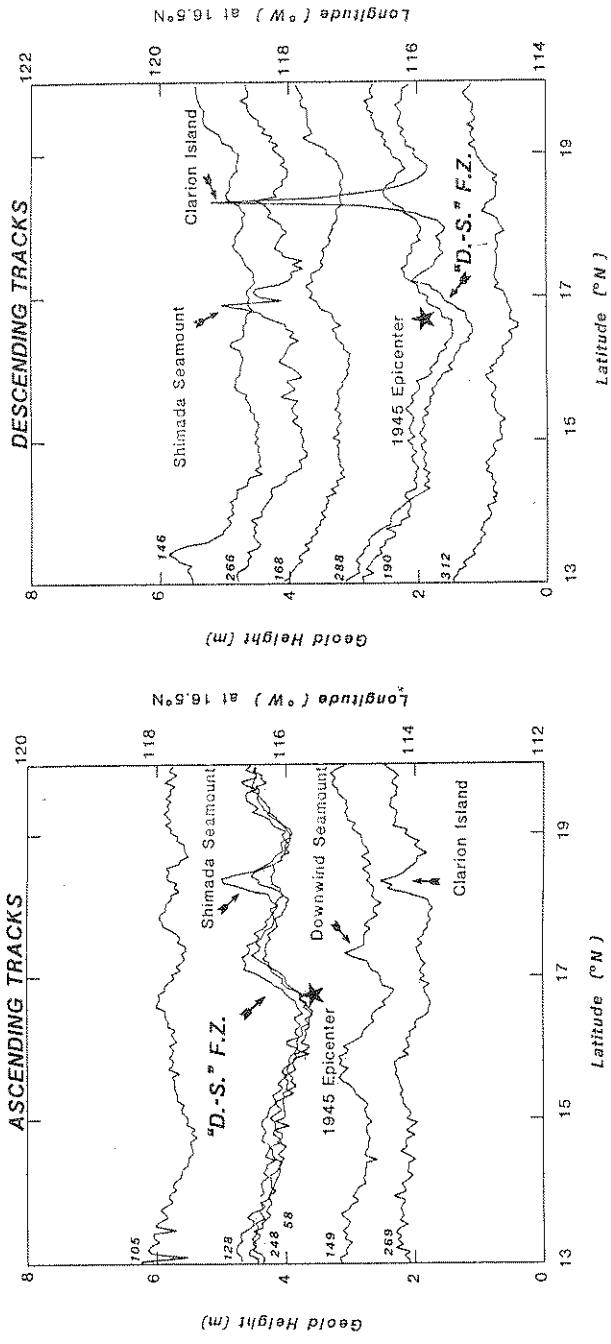

Fig. 12. Residual geoid height along selected SEASAT tracks in the area of the 1945 epicenter (left: ascending tracks; right: descending tracks). Linear trend over range of latitudes plotted has been subtracted from data. Numbers at left identify tracks (see Fig. 9). Each track is offset linearly in longitude. Note consistent signature of proposed Downwind–Shimada ("D–S") Fracture Zone.

The 1973 event ($m_b = 4.7$) also maps along the Downwind–Shimada FZ. The 1985 event ($m_b = 4.7$) is located in the prolongation of the Downwind–Shimada FZ, but in an area where its signature has vanished from the geoid.

The tentative locations of the 1930 earthquake, and the well-located 1985 and 1986 epicenters fall along the line separating, on present-day Pacific plate, lithosphere generated at the Guadalupe–Pacific Ridge and at the Mathematicians Ridge. Such borders have been tentatively identified elsewhere as lines of weakness, where seismicity can be preferentially sited (Okal and Bergeal, 1983). Among the scattered epicenters revealed by our wide scale search, the 1961 earthquake relocates to the vicinity of the Siqueiros FZ, and the 1977 earthquake to the fossil Farallon Ridge segment between the Galápagos and Siqueiros FZs. The other epicenters cannot be associated with known bathymetric features. The level of correlation between these earthquake epicenters and topographic features is in line with worldwide results (Bergman and Solomon, 1980; Okal, 1983).

4. Discussion

Previous studies have suggested several processes which can cause concentration of normal faulting seismicity in oceanic lithosphere. Such earthquakes have been commonly found in the younger parts of oceanic plates (Wiens and Stein, 1984; Bergman and Solomon, 1984) and recent models such as Bratt et al.'s (1985) have interpreted them as the release of thermal stresses due to the rapid cooling of the plate as it moves away from the ridge. Alternatively, concentrations of large 'intraplate' earthquakes, some of them featuring normal faulting, can represent deformation along a diffuse plate boundary, e.g., in the Indian Ocean (Wiens et al., 1985). Finally, intraplate volcanism has been known to cause swarms of normal faulting earthquakes (e.g. the 1968 Fernandina caldera collapse (Filson et al., 1973).

Evidence suggesting that thermoelastic stresses may be important sources of seismicity in the young oceanic lithosphere includes the decrease in the intraplate seismicity rate with lithospheric age (Wiens and Stein, 1983), and the agreement of the inferred stress orientations and depths of intraplate earthquakes in young lithosphere with the predictions of thermoelastic stress calculations (Turcotte, 1974; Bergman and Solomon, 1984; Wiens and Stein, 1984; Bratt et al., 1985). The Eastcentral Pacific events show several similarities to the young lithosphere events generally associated with thermoelastic stress. Klitgord and Mammerickx's (1982) magnetic anomaly identifications, interpreted in the chronology of Harland et al. (1982), show that the earthquakes occurred in lithosphere of ages 18 and 15 Ma. Also, the earthquakes are located at mantle depths (12–15 km), where the greatest tensional stresses are predicted.

Turcotte (1974) suggests that thermoelastic stress should give rise to tensional stresses oriented parallel to isochrones (i.e. parallel to the spreading ridge and perpendicular to the trend of fracture zones). Systematic surveys show that the tensional axes of intraplate earthquakes in young oceanic lithosphere are preferentially aligned in this direction, although a large scatter is observed (see Fig. 5 of Wiens and Stein (1984)). In the case of the 1945 event, the orientation of the tensional axis (N10° W) is nearly parallel to the isochrones, and thus to the predicted direction of thermoelastic stress. The location of the 1945 event along the geoid feature tentatively identified as a fracture zone suggests that it may represent a perfect example of the thermal crack model of fracture zones (Turcotte, 1974; Sandwell, 1986). The tensional axes of the 1984–1986 swarm events (~ N40° W) show a greater deviation from the predicted direction of thermal stress; however, this deviation is well within the scatter found for other events in young lithosphere. Thus, it is in principle possible to propose thermoelastic stress as a mechanism for the Eastcentral Pacific events.

However, there are difficulties with applying the thermoelastic stress model to the Eastcentral Pacific. First, as illustrated by the mere size of the earthquakes, this seismicity adds up to an abnormally high seismic moment release: the 1984 mainshock studied here is itself one of the largest oceanic intraplate events since the advent of the WWSSN network. Among normal faulting oceanic intraplate earthquakes, only the 1983 Chagos

event was larger than the 1945 shock, and an event near Deception Island in 1971 comparable in size; both of those were clearly associated with processes other than thermal stresses: the former with the diffuse Indian Ocean boundary, the latter occurred within a major rift zone (Pelayo and Wiens, 1986). The concentration of large events within a small region observed in the Eastcentral Pacific is difficult to explain using thermoelastic stresses, which should be relatively uniformly distributed owing to the uniformity of the temperature of the oceanic lithosphere. Furthermore, the highest concentration of thermoelastic stress should be in the youngest lithosphere. For instance, Bratt et al.'s (1985) model shows that stresses in very young lithosphere should be several times the stresses in lithosphere of age 15–20 Ma; indeed in other oceanic provinces, most near-ridge seismicity occurs in lithosphere younger than 15 Ma, while in the Eastcentral Pacific events occur in lithosphere of age 15 and 18 Ma.

With this remark in mind, we first address the question whether the intense 1984–1985 could be due to a burst of intraplate volcanism. Although it is difficult to totally rule out this possibility, several lines of evidence argue against it.

First, no topographic feature is known at the location of the 1984 swarm, either from shipboard bathymetry or from satellite altimetry. While large normal faulting earthquakes occasionally occur as part of documented volcanic episodes, these have been interpreted as expressing the tectonic readjustment of large volcanic edifices, either islands or large seamounts showing up prominently in the geoid. No such feature is known in the epicentral area of the 1984 swarm. Furthermore, swarms associated with volcanism typically have anomalous frequency–magnitude relations, with b values ranging from 1.4 to more than 3 (McNutt, 1983), whereas our 1984 swarm had a b value of 1.05 ± 0.26. However, this b value alone should not be taken as a definite proof against a volcanic nature of the swarm: the earthquakes recorded at a teleseismic distance could conceivably represent the final, 'tectonic', stage of a major volcanic swarm whose magmatic events featuring the increased b value, but being of a lower magnitude, would have escaped detection (see, for example, Talandier and Okal (1984) for a discussion in the case of a well-documented volcanic swarm). Finally, the alignment of the major, well-located, events of the swarm along one of the fault planes determined from the focal mechanism study argues strongly for a tectonic process.

Other concentrations of intraplate seismicity are apparently related to regions of enhanced tectonic stress or regions of preferred stress release. Okal et al. (1980) suggest that concentrations of smaller magnitude seismicity in the south-central Pacific released 'ridge-push' stresses. Seismicity on the Cocos plate west of the Panama Fracture Zone, including a swarm in March, 1976 (Wiens and Stein, 1984) may be related to diffusion of strike-slip motion from the Panama Fracture Zone to 'inactive' fracture zones to the west. Okal et al. (1986) have interpreted the seismicity at the site of the Gilbert Islands swarm as due to the early stages of the reorganization of the Southwest Pacific subduction zone. However, in none of these cases has the seismicity featured the release of horizontal tensional stresses.

Another possibility would be to associate the earthquake concentration in the Eastcentral Pacific with major, plate-wide, processes, such as diffuse plate boundaries, as exemplified by the seismicity of the Indian Ocean near the Ninetyeast Ridge and Chagos Bank (Stein, 1978; Stein and Okal, 1978; Wiens, 1986). (Earthquake concentrations in the Caroline Basin region (Weissel and Anderson, 1978; Hegarty et al., 1983) and in the Atlantic Ocean between the Caribbean plate and the Mid-Atlantic Ridge (Stein et al., 1982) also appear to result from tectonic deformation associated with diffuse plate boundaries.) However, our systematic search of intraplate seismicity in neighboring areas has failed to document any potential plate-wide process, and emphasized the limited extent of this region of concentrated seismicity. In this respect, this area differs substantially from the region bordering the Southeast Indian Ridge in the Indian plate, whose enhanced normal faulting seismicity has been successfully explained in terms of plate-wide processes, such as stress perturbations in the Australian plate (Cloetingh and Wortel, 1985) or thermoelastic stresses (Bratt et al., 1985).

In conclusion, the most important result of this study is the concentration of large normal faulting earthquakes in the Eastcentral Pacific, a pattern previously observed only in the Indian Ocean. The tectonic significance of these earthquakes remains uncertain. While their individual mechanisms can be explained from thermoe stic stresses, their apparent concentration within a region a few hundred kilometers in dimension may indicate that such earthquakes result from localized stress perturbations from as yet undiscovered sources. Alternatively, they may indicate that the effect of thermoelastic stresses on seismicity is modified by local stress perturbations which tend to concentrate earthquakes within small regions, or that the release of thermoelastic stress is extremely non-uniform and synchronized in time over regions on the scale of hundreds of kilometers. Further analysis of current and historical oceanic intraplate seismicity will be necessary for a more definitive interpretation.

Acknowledgments

We thank the many people who aided this study by supplying earthquake records, particularly Zenon Jimenez (Instituto de Geofisica), Cinna Lomnitz (RESMAC), Joan Gomberg (UCSD), Jim Newberry (USGS), Bruce Bolt (UC Berkeley), Brian Ferris (Wellington), Rev. James McCaffrey (Weston Observatory), and Rev. Ramon Cabré (La Paz). We are also grateful to Kien Dominh and Anny Cazenave, who provided the SEASAT dataset used in this study. This research was supported by the National Science Foundation, under Grant EAR-86-18044 (DAW), and the Office of Naval Research, under Contract N00014-84-C-0616 (EAO). Acknowledgment is made to the donors of the Petroleum Research Fund, administered by the American Chemical Society, for partial support of this research under Grants 1729-ACZ (EAO) and 16780-GZ (DAW).

References

Aki, K., 1965. Maximum likelihood estimate of b in the formula $\log N = a - bM$, and its confidence limits. Bull. Earthq. Res. Inst. Univ. Tokyo, 43: 237–239.

Bergman, E.A. olomon, S.C., 1980. Oceanic intraplate earthquakes: ations for local and regional intraplate stress. J. Ge Res., 85: 5389–5410

Bergman, E.A. a omon, S.C., 1984. Source mechanisms of earthquakes nid-ocean ridges from body waveform inversion, ir ions for the early evolution of oceanic lithosphere. phys. Res., 89: 11415–11441.

Bergman, E.A. olomon, S.C., 1985. Earthquake source mechanisms body-waveform inversion and intraplate tectonics in orthern Indian Ocean. Phys. Earth Planet. Inter., 40: 1

Bergman, E.A. ólek, J.L. and Solomon, S.C., 1984. An extensive re f off-ridge normal faulting earthquakes in the southe ndian Ocean. J. Geophys. Res., 89: 2425–2443.

Bratt, S.R., Bergman, E.A. and Solo n, S.C., 1985. Thermoelastic stress: how important as a use of earthquakes in young lithosphere? J. Geophys. Res., 90: 10249–10260.

Cazenave, A. and Okal, E.A., 1986. Use of satellite altimetry in studies of the oceanic lithosphere. In: A.J. Anderson and A. Cazenave (Editors), Space Geodesy and Geodynamics. Academic Press, London, pp. 347–375.

Chase, T.E., Menard, H.W. and Mammerickx, J., 1970. Bathymetry of the North Pacific. Scripps Inst. Oceanogr., San Diego (Map).

Cloetingh, S. and Wortel, R., 1985. Regional stress field of the Indian plate. Geophys. Res. Lett., 12: 77–80.

Dziewonski, A.M., Franzen, J.E. and Woodhouse, J.H., 1985. Centroid moment tensor solutions for October–December, 1984. Phys. Earth Planet. Inter., 39: 147–156.

Filson, J., Simkin, T. and Leu, L., 1973. Seismicity of a caldera collapse: Galápagos Islands, 1968. J. Geophys. Res., 78: 8591–8622.

Flinn, E.A., 1965. Confidence regions and error determinations for seismic event location. Rev. Geophys., 3: 157–185.

Francis, T.J.G., 1974. A new interpretation of the 1968 Fernandina Caldera collapse and its implications for the mid-ocean ridges. Geophys. J.R. Astron. Soc., 39: 301–318.

Gutenberg, B. and Richter, C.F., 1954. Seismicity of the Earth and Associated Phenomena. Princeton University Press, Princeton, N.J.

Harland, W.B., Cox, A.V., Llewellyn, P.G., Pickton, C.A.G., Smith, A.G. and Walters, R., 1982. A Geologic Time Scale. Cambridge University Press, New York.

Hegarty, K.A., Weissel, J.K. and Hayes, D.E., 1983. Convergence at the Caroline-Pacific plate boundary: collision and subduction. In: D.E. Hayes (Editor), The Tectonic and Geologic Evolution of southeast Asian Seas and Islands, part 2. Am. Geophys. Union, Washington, Geophys. Mon., 27: 326–348.

Kanamori, H. and Anderson, D.L., 1975. Theoretical basis of some empirical relations in seismology. Bull. Seismol. Soc. Am., 65: 1073–1095.

Kanamori, H. and Stewart, G.S., 1976. Mode of strain release along the Gibbs Fracture Zone, Mid-Atlantic Ridge. Phys. Earth Planet. Inter., 11: 312–332.

Kaufman, K. and Burdick, L.J., 1980. The reproducing earthquakes of the Galapagos Islands. Bull. Seismol. Soc. Am., 70: 1759–1770.

Klitgord, K.D. and Mammerickx, J., 1982. Northern East Pacific Rise: magnetic anomaly and bathymetric framework. J. Geophys. Res., 87: 6725–6750.

Kikuchi, M. and Kanamori, H., 1982. Inversion of complex body waves. Bull. Seismol. Soc. Am., 72: 491–506.

Langston, C.A. and Helmberger, D.V., 1975. A procedure for modelling shallow dislocation sources. Geophys. J.R. Astron. Soc., 42: 117–130.

Lay, T. and Okal, E.A., 1983. The Gilbert Islands (Republic of Kiribati) earthquake swarm of 1981–1983. Phys. Earth Planet. Inter., 33: 284–303.

Mammerickx, J. and Klitgord, K.D., 1982. Northern East Pacific Rise: evolution from 25 m.y.b.p. to the present. J. Geophys. Res., 87: 6751–6759.

Mammerickx, J. and Smith, S.M., 1982. General Bathymetric Chart of the Oceans (GEBCO), Sheet 5.07. Canadian Hydrographic Service, Ottawa.

McNutt, S.R., 1983. A review of volcano seismicity. EOS, Trans. Am. Geophys. Union, 64: 265 (abstract).

Okal, E.A., 1983. Oceanic intraplate seismicity. Annu. Rev. Earth Planet. Sci., 11: 195–214.

Okal, E.A., 1984. Intraplate seismicity of the southern part of the Pacific Plate. J. Geophys. Res., 89: 10053–10071.

Okal, E.A. and Bergeal, J.-M., 1983. Mapping the Miocene Farallon Ridge jump on the Pacific plate: a seismic line of weakness. Earth Planet. Sci. Lett., 63: 113–122.

Okal, E.A., Talandier, J., Sverdrup, K.A. and Jordan, T.H., 1980. Seismicity and tectonic stress in the south-central Pacific. J. Geophys. Res., 85: 6479–6495.

Okal, E.A., Woods, D.F. and Lay, T., 1986. Intraplate deformation in the Samoa–Gilbert–Ralik area: a prelude to a change of plate boundaries in the Southwest Pacific? Tectonophysics, 132: 69–78.

Pelayo, A.M. and Wiens, D.A., 1986. Seismotectonics of the western Scotia Plate region. EOS, Trans. Am. Geophys. Union, 67: 1239 (abstract).

Sandwell, D.T., 1986. Thermal stress and the spacings of transform faults. J. Geophys. Res., 91: 6405–6417.

Stein, S., 1978. An earthquake swarm on the Chagos–Laccadive Ridge and its tectonic implications. Geophys. J.R. Astron. Soc., 55: 577–588.

Stein, S. and Okal, E.A., 1978. Seismicity and tectonics of the Ninetyeast Ridge area: evidence for internal deformation of the Indian plate. J. Geophys. Res., 83: 2233–2245.

Stein, S. and Wiens, D.A., 1986. Depth determination for shallow teleseismic earthquakes: methods and results. Rev. Geophys., 24: 806–832.

Stein, S., Engeln, J.F., Wiens, D.A., Fujita, K. and Speed, R.C., 1982. Subduction seismicity and tectonics in the Lesser Antilles arc. J. Geophys. Res., 87: 8642–8664.

Stein, S., Okal, E.A. and Wiens, D.A., 1987. Application of Modern Techniques to Analysis of Historical Earthquakes. Proc. Int. Symp. Historical Earthquake: XXIIIrd General Assembly IASPEI, Tokyo, August 1985, in press.

Sykes, L.R., 1970. Earthquake swarms and sea-floor spreading. J. Geophys. Res., 75: 6598–6611.

Talandier, J. and Okal, E.A., 1984. The volcanoseismic swarms of 1981–1983 in the Tahiti–Mehetia area, French Polynesia. J. Geophys. Res., 89: 11216–11234.

Turcotte, D.L., 1974. Are transform faults thermal contraction cracks? J. Geophys. Res., 79: 2573–2577.

Weissel, J.K. and Anderson, R.N., 1978. Is there a Caroline Plate? Earth Planet. Sci. Lett., 41: 143–158.

Wiens, D.A., 1985. Oceanic Intraplate Seismicity: Implications for the Rheology and Tectonics of the Oceanic Lithosphere. Ph.D. Thesis, Northwestern Univ., Evanston, Illinois, 220 pp.

Wiens, D.A., 1986. Historical seismicity near Chagos: a complex deformation zone in the equatorial Indian Ocean. Earth Planet. Sci. Lett., 76: 350–360.

Wiens, D.A. and Stein, S., 1983. Age dependence of oceanic intraplate seismicity and implications for lithospheric evolution. J. Geophys. Res., 88: 6455–6458.

Wiens, D.A. and Stein, S., 1984. Intraplate seismicity and stresses in young oceanic lithosphere. J. Geophys. Res., 89: 11442–11464.

Wiens, D.A., DeMets, D.C., Gordon, R.G., Stein, S., Argus, D.F., Engeln, J.F., Lundgren, P.R., Quible, D., Stein, C., Weinstein, S. and Woods, D.F., 1985. A diffuse plate boundary model for Indian Ocean tectonics. Geophys. Res. Lett., 12: 429–432.